

**COMPUTATIONAL DESIGN AND INVESTIGATION  
OF NEW BENZOPHENONES AND BENZOPHENONE  
IMINES INHIBITORS FOR BREAST CANCER**

by

**AMNEH MOHAMMAD SHTAIWI**

**Thesis submitted in fulfillment of the requirements  
for the degree of  
Doctor of Philosophy**

**October 2018**

## ACKNOWLEDGEMENT

بِسْمِ اللَّهِ الرَّحْمَنِ الرَّحِيمِ

﴿يَرْفَعِ اللَّهُ الَّذِينَ آمَنُوا مِنْكُمْ وَالَّذِينَ أُوتُوا الْعِلْمَ دَرَجَاتٍ وَاللَّهُ بِمَا تَعْمَلُونَ خَبِيرٌ﴾

صَدَقَ اللَّهُ الْعَظِيمُ

*In the Name of Allah, the Most Merciful, the Most Compassionate all praise be to Allah, the Lord of the worlds; and prayers and peace be upon Mohamed His servant and messenger. First and foremost, I must acknowledge my limitless thanks to Allah; the Ever-Thankful, for the strengths and His blessing in completing this thesis. I am totally sure that this work would have never become true, without His guidance. I would like to express the deepest appreciation to my beloved supervisor, Prof. Dr. Rohana Adnan for her supervision and constant support. Her invaluable help of constructive comments and suggestions throughout the experimental and thesis works have contributed to the success of this research. Not forgotten, my appreciation to my co-supervisor, Dr Melati Khairuddean for her support and knowledge regarding this topic. I also owe a deep debt of gratitude to our university USM for giving us the financial support through the Fellowship Scheme under the Institute of Postgraduate Studies to complete this work.*

*Special appreciation goes to my husband, Musa Ismail, whose constant encouragement, limitless giving and great sacrifice, helped me accomplish my degree. My wholehearted thanks to my family, Father and Mother, for their continuous love, support, patience and understanding and for their prayers. Not forgotten, my special gratitude goes to my lovey kids Anas, Raghad and Yaman for their generous support they provided me throughout my entire life and particularly through the process of pursuing the Ph.D degree.*

*I would like to take this opportunity to say warm thanks to all my beloved group members, Shikin, Zuhir, Farah, Fitrah, Nazihah, Solehah and Saifullahi who have been so supportive along the way. I also wish to thanks to all staff in School of Chemical Sciences, especially, Mr. Nizam and Mr. Azizo for the many kind helps, technical assistance provided, comments and motivational supports during my study. May Allah bless all of you.*

## TABLE OF CONTENTS

Acknowledgement	ii
Table of Contents	iii
List of Tables	vi
List of Figures	viii
List of Abbreviations	xiv
List of Symbols	xvii
Abstrak	xix
Abstract	xxi
<b>CHAPTER 1 - INTRODUCTION</b>	<b>1</b>
1.1 Breast Cancer	1
1.2 Problem Statement	3
1.3 Aims of the Study	4
<b>CHAPTER 2 - LITERATURE REVIEW</b>	<b>5</b>
2.1 The Estrogen Receptor: Structures and the Mechanism of Action	5
2.1.1 Estrogen and the Estrogen Receptor (ER)	5
2.1.2 The Mechanism of Action of the Estrogen Receptor	13
2.1.3 The Mechanism of Action of the Estrogen Receptor	13
2.2 Agonists and Antagonists of the Estrogen Receptor	15
2.2.1 Full and Partial Agonists	15
2.2.2 Partial Antagonist as Selective Estrogen Receptor Modulators	16
2.2.3 Full Antagonist	22
2.3 Antiestrogen Resistance	24

2.4	Benzophenones and Imines Derivatives as Estrogen Receptor Inhibitors	26
2.4.1	Benzophenones Derivatives	26
2.4.2	Benzophenone Imines	28
2.5	Computational Methods	29
2.5.1	Molecular Docking	29
2.5.2	Molecular Dynamics Simulation	33
2.5.3	Free Energy Calculations	38
2.6	Applications of Computational Methods	40
<b>CHAPTER 3 - MATERIALS AND METHODS</b>		48
3.1	Technical Details	48
3.2	Work Flow	49
3.3	Strategies for the Design of New Benzophenone Imines	51
3.4	Molecular Preparations of the hER $\alpha$ Structures and Ligands	53
3.5	Molecular Docking	54
3.6	Molecular Dynamics Simulation	56
3.7	Trajectory Analysis	58
<b>CHAPTER 4 - RESULTS AND DISCUSSION</b>		61
4.1	Structures of Human Estrogen Receptors	61
4.2	Molecule Structures of Benzophenones and Benzophenone Imines	63
4.3	Lipinski's Rule of Five	66
4.4	Molecular Docking Study	66
4.4.1	Docking Studies of Benzophenones and Morpholine Ether Derivatives	67
4.4.2	Docking Studies of Benzophenone Imines	72

4.4.2.(a)	Docking Studies of Benzophenone Imines with Apo hER $\alpha$	73
4.4.2.(b)	Docking Studies of Benzophenone Imines with Antagonist hER $\alpha$	81
4.4.2.(c)	Docking Studies of Benzophenone Imines with Agonist hER $\alpha$	88
4.5	Molecular Dynamics Simulation	91
4.5.1	Structural Stability of apo hER $\alpha$ Free and Complex with <b>4b</b>	91
4.5.1.(a)	Transition Paths Analysis of H12 in Dimer Form	98
4.5.1.(b)	Free Energy Analysis of hER $\alpha$ -4b Monomer and Dimer Complexes	100
4.5.2	Molecular Dynamics simulation of Apo, Antagonist and Agonist of hER $\alpha$ with Benzophenone Imine <b>5c</b>	104
4.5.2.(a)	Root Mean Square Deviation	105
4.5.2.(b)	Radius of Gyration	107
4.5.2.(c)	Root Mean Square Fluctuation	109
4.5.2.(d)	Transition Paths Analysis of Apo, Antagonist and Agonist Systems	112
4.5.2.(e)	Hydrogen Bond Analysis	117
4.5.2.(f)	Distance Analysis	121
4.5.3	Free Energy Calculations	123

## CHAPTER 5 - CONCLUSIONS

5.1	Conclusions	131
5.2	Future Recommendations of Current Work	133

REFERENCES	134
------------	-----

## APPENDICES

## LIST OF PUBLICATIONS AND CONFERENCE PRESENTATIONS

## LIST OF TABLES

	Page
Table 2.1	21
Table 2.2	24
Table 2.3	43
Table 2.4	44
Table 3.1	56
Table 3.2	57
Table 4.1	63
Table 4.2	66
Table 4.3	68
Table 4.4	74
Table 4.5	80

Table 4.6	Binding free energies, $\Delta G_b$ , inhibition constants, $K_i$ and cluster number of antagonist monomer 3ERT hER $\alpha$ conformation interacting with 4-OHT and benzophenones imines, (1-8)c	81
Table 4.7	Hydrogen bonds formation, bond length and hydrophobic residues of antagonist monomer 3ERT hER $\alpha$ conformation interacting with 4-OHT and BIs. (see Appendices 1 for atoms labelling)	85
Table 4.8	Binding free energies, $\Delta G_b$ , inhibition constants, $K_i$ and cluster number of agonist monomer 1G50 hER $\alpha$ conformation interacting with E2 and benzophenones imines (1-8)c	90
Table 4.9	The four different models in 60 ns MD simulations of apo ER $\alpha$ 1A52	91
Table 4.10	The total binding energy and its components of monomer and dimer <b>1ap_c</b> and <b>2ap_c</b> complexes obtained from <i>g_mmpbsa</i>	101
Table 4.11	The six models used in 100 ns MD simulations of apo monomer 1A52, antagonist 3ERT and agonist 1G50	104
Table 4.12	H-bond occupancy between the amino acid residues of hER $\alpha$ and ligand <b>5c</b> in the three systems	118
Table 4.13	Calculated binding free energy and its components based on MM-GBSA method for the three hER $\alpha$ - <b>5c</b> complexes	124
Table 4.14	Comparison of the calculated ( $\Delta G_{calc}$ ) and experimental ( $\Delta G_{exp}$ ) total binding free energies values (in kJ/mol) for E2 and 4-OHT complexed with hER $\alpha$ with the hER $\alpha$ - <b>5c</b> complexes	125

## LIST OF FIGURES

		Page
Figure 2.1	The major biosynthetic paths of endogenous Estrone (E1) and 17 $\beta$ -estradiol (E2) (Larionov et al., 2003). Figure was generated using ChemDraw16 software	6
Figure 2.2	The human estrogen receptor $\alpha$ and $\beta$ (hER $\alpha$ and hER $\beta$ ). Where A/B is the N-terminal domain, C is the DNA binding domain, D is the hinge domain and E/F C-terminal domain	7
Figure 2.3	Binding mode of 17 $\beta$ -estradiol in ER $\alpha$ (PDB:1G50) (Brzozowski et al., 1997). Figure was generated using Chimera 1.11.2 software	9
Figure 2.4	(a) Backbone of agonist conformation of ER $\alpha$ LBD (PDB: 1G50) in complex with estradiol E2 (cyan stick). (b) Antagonist conformation of ER $\alpha$ LBD (PDB: 3ERT) in complex with 4-OHT (grey stick). Important helices are highlighted: H3 (blue), H5 (orange), H6 (grey), H11 (green) and H12 (red). Figure was generated using Chimera 1.11.2 software	11
Figure 2.5	Backbone of apo conformation of ER $\alpha$ LBD (PDB ID: 1A52) in complex with estradiol (yellow). Figure was generated using Chimera 1.11.2 software	12
Figure 2.6	Mechanism of action of estrogen dependant gene transcription in cancer cell (Batista & Martínez, 2013)	14
Figure 2.7	Structures of selected full and partial agonists ligands against ER $\alpha$ LBD. Figure was generated using ChemDraw 16 software	15
Figure 2.8	Structures of selected ER $\alpha$ partial antagonists as SERMs. Figure was generated using ChemDraw 16 software	16
Figure 2.9	Binding mode of 4-hydroxytamoxifen 4-OHT in ER $\alpha$ , PDB: 3ERT (Park & Jordan, 2002). Figure was generated using Chimera 1.11.2 software	17
Figure 2.10	Binding mode of raloxifene (grey stick) in ER $\alpha$ , PDB: 1ERR (Jordan, 2003a). Figure was generated using Chimera 1.11.2 software	18
Figure 2.11	Timeline of the major estrogen, antiestrogens and SERMs for the treatment and prevention of breast cancer and osteoporosis (Maximov et al., 2013)	20
Figure 2.12	Structures of selected ER $\alpha$ pure antagonists (Wakeling et al., 1991). Figure was generated using ChemDraw 16 software	22
Figure 2.13	Binding mode of ICI 164,384 (grey stick) in ER $\beta$ , PDB: 1HJI (Pike et al., 2001). Figure was generated using Chimera 1.11.2 software	23

Figure 2.14	Chemical structures of (a) benzophenone (b) meta-imidazolylmethyl benzophenones and (c) 2,4-dihydroxy benzophenone. Figure was generated using ChemDraw 16 software	27
Figure 2.15	Chemical structure of benzophenone imines (BIs). Figure was generated using ChemDraw 16 software	29
Figure 2.16	Chemical structure of chalcone derivatives (Muchtaridi et al., 2017). Figure was generated using ChemDraw 16 software	33
Figure 2.17	Graphic illustrations of force field interactions, covalent bonds are indicated by heavy solid lines, nonbonded interactions by a dashed line. Where $b$ is the bond length, $\theta$ is the bond angle, $\phi$ is the dihedral angle and $r_{ij}$ is the position	37
Figure 2.18	Chemical structures of some EDCs bisphenols (Cao et al., 2017). Figure was generated using ChemDraw 16 software.	42
Figure 2.19	Chemical structures of selected ER ligands (Liu & Mooney, 2011)	45
Figure 2.20	Chemical structures of (a) S-allylmercaptocysteine (b) 5-hydroxy-L- tryptophan. Figure was generated using ChemDraw 16 software	47
Figure 3.1	Summary of the flow of work conducted	50
Figure 3.2	The design of novel triarylimine family. Figure was generated using ChemDraw 16 software	52
Figure 3.3	Chemical structures of the newly designed ligands, natural E2 and synthetic 4-OHT substrates used in this study, where X from (1-4) are substituted groups H, F, Cl and OH, respectively, Y from (1-5) are substituted groups H, F, Cl, CH <sub>3</sub> and OH, respectively. Figure was generated using ChemDraw 16 software	55
Figure 4.1	Backbone of (a) apo dimer conformation of ER $\alpha$ LBD (PDB: 1A52) in complex with estradiol (yellow) (b) Agonist monomer conformation of ER $\alpha$ LBD (PDB: 1G50) in complex with estradiol (cyan) (c) Antagonist monomer conformation of ER $\alpha$ LBD (PDB: 3ERT) in complex with 4-OHT (grey) Important helices are highlighted: H3 (blue), H5 (orange), H6 (grey), H11 (green) and H12 (red) (Pike et al., 1999; Tanenbaum et al., 1998). Figure was generated using Chimera 1.11.2 software	62

Figure 4.2	The docking poses of 17 $\beta$ -estradiol with apo dimer 1A52 hER $\alpha$ , cyan stick, superimpose with the (a) benzophenones derivatives 4a (orange), (b) morpholine ether benzophenones, 4b, (green). Figure was generated using Chimera 1.11.2 software	70
Figure 4.3	Hydrogen bonds formation and hydrophobic residues interactions of the protein-ligand interactions for estradiol E2, hydroxyl derivative benzophenone 4a and hydroxyl derivative of morpholine ether benzophenones 4b using Ligplot software	71
Figure 4.4	Diagram drawn based on the crystal structure of the hER $\alpha$ -LBD complex with E2 (black) and 4-OHT (red). The amino acids that interact with the E2 and 4-OHT and the hydrogen bonding formation are shown. The difference between E2 and the antiestrogen 4-OHT is the interaction with Asp351	72
Figure 4.5	Overlay of the crystal structure of 4-OHT (red) with benzophenone imines (black) (a) 1c (b) 8c. Figures was generated using ChemDraw 16 software	73
Figure 4.6	Superimposition of 100 conformations of E2 docked in the same orientation in the apo dimer 1A52 hER $\alpha$ binding pocket. Hydrogen bonding with the important bonds length are highlighted. Figure was generated using Chimera 1.11.2 software.	75
Figure 4.7	Superimposition of 100 conformations of 4-hydroxy tamoxifen 4-OHT docked in the same orientation in the apo dimer 1A52 hER $\alpha$ binding pocket. Hydrogen bonding formations for the best candidate from docking results are highlighted	76
Figure 4.8	Diagram showing the binding mode of the (a) E2 (black) overlay with 4-OHT (red), (b) E2 (black) overlay with raloxifene (red) in the hER $\alpha$ -LBD complex. The amino acids that interact with the E2 and SERMs and the hydrogen bonding formation are shown. Figure was generated using ChemDraw 16 software	77
Figure 4.9	Superimposition of the 100 conformation of 5c docked in the binding pocket of apo dimer 1A52 hER $\alpha$ -5c complex. Hydrogen bonding formations for the best candidate from docking results are highlighted. Figure was generated using Chimera 1.11.2 software	77
Figure 4.10	Superimpose of 100 conformations for BIs, 1-8c, docked orientation in apo dimer 1A52 LBD. Important amino acid residues are highlighted. Figure was generated using Chimera 1.11.2 software	79

Figure 4.11	Superimpose of the 100 conformations of 4-OHT docked in the same orientation in the antagonist monomer 3ERT hER $\alpha$ -LBD. Hydrogen bonding formations for the best candidate from docking results are highlighted	82
Figure 4.12	Superimpose of the 100 conformations of <b>5c</b> docked in the same orientation in the antagonist monomer 3ERT hER $\alpha$ LBD. Hydrogen bonding formations for the best candidate from docking results are highlighted. Figure was generated using Chimera 1.11.2 software	83
Figure 4.13	Superimpose of the 100 conformations of <b>4c</b> docked in the same orientation in the antagonist monomer 3ERT hER $\alpha$ LBD. Hydrogen bonding formations for the best candidate from docking results are highlighted. Figure was generated using Chimera 1.11.2 software	83
Figure 4.14	Superimpose of 100 conformations for BIs, <b>1-8c</b> , docked in antagonist monomer 3ERT hER $\alpha$ -LBD. Figure was generated using Chimera 1.11.2 software.	87
Figure 4.15	Superimpose of 100 conformations of E2 (stick) docked in the agonist monomer 1G50 hER $\alpha$ binding site (ribbon). Hydrogen bonding formation are also highlighted. Figure was generated using Chimera 1.11.2 software	89
Figure 4.16	Superimpose of 100 conformations of <b>5c</b> docked in the agonist monomer 1G50 binding site. Important helices highlighted are: H3 (blue), H6 (grey), H11 (green) and H12 (red). Figure was generated using Chimera 1.11.2 software	89
Figure 4.17	The RMSDs of all backbone atoms of the apo hER $\alpha$ LBD throughout simulations for (a) <b>1ap</b> and <b>1ap_c</b> , (b) <b>2ap</b> and <b>2ap_c</b> . Figure was generated using xmgrace software	93
Figure 4.18	Variation of radius of gyration, $R_g$ , of the apo hER $\alpha$ LBD for (a) <b>1ap</b> and <b>1ap_c</b> , (b) <b>2ap</b> and <b>2ap_c</b> . Black and red lines represent free and complex conformations of hER $\alpha$ , respectively. Figure was generated using xmgrace software	94
Figure 4.19	RMSF profiles of the apo hER $\alpha$ LBD (a) monomer forms, <b>1ap</b> and <b>1ap_c</b> , and (b) dimer forms, <b>2ap</b> and <b>2ap_c</b> . Black and red lines represent free and complex conformation of hER $\alpha$ , respectively. Figure was generated using xmgrace software	96
Figure 4.20	Snapshot obtained for morpholine ether BP (green) at 60 ns superimpose with the crystal structure of 17 $\beta$ -estradiol (orange), pdb: 1A52, hydrogen bonds are represented in black dashed lines. Figure was generated using PyMOL software	97

Figure 4.21	Variations in the number of hydrogen bonds between apo hER $\alpha$ LBD bound with 4b in (a) <b>1ap_c</b> , monomer complex, (b) <b>2ap_c</b> , dimer complex and (c) hydrogen bonds between Glu353 with 4b. Figure was generated using xmgrace software	98
Figure 4.22	The minimum distance analysis between chain <b>A</b> and chain <b>B</b> of H12 of apo hER $\alpha$ LBD. Black and red lines represent the free and dimer complex conformations, respectively.	99
Figure 4.23	Overlay of snapshots of the conformational dynamics of (a) free <b>2ap</b> and (b) dimer complex <b>2ap_c</b> . For the H12 snapshots, red after 1 ns, green after 30 ns, and magenta at 60 ns. Important helices in the binding cavity are highlighted	99
Figure 4.24	Total binding free energy of monomer and dimer, <b>1ap_c</b> and <b>2ap_c</b> complexes calculated by g_mmpbsa tool. Black and red lines represent monomer and dimer complexes, respectively. Figure was generated using xmgrace software	101
Figure 4.25	Energetic contributions of apo hER $\alpha$ residues. The mapping of energy contribution on the structure of (a) <b>1ap_c</b> complex. (b) <b>2ap_c</b> complex. The energy mappings are prepared using energy2bfac. Figure was generated using VMD software	102
Figure 4.26	The energy contributions of amino acid of apo hER $\alpha$ complex (a) Monomer, <b>1ap_c</b> and (b) Dimer, <b>2ap_c</b> with morpholine ether BP, <b>4b</b> . Figure was generated using xmgrace software	103
Figure 4.27	The RMSDs of all backbone atoms of the apo hER $\alpha$ LBD throughout 100 ns MD simulations for (a) <b>3ap</b> and <b>3ap_c</b> , (b) <b>4an</b> , <b>2an_c</b> and (c) <b>5ag</b> , <b>ag_c</b> . Figure was generated using xmgrace software	106
Figure 4.28	The Rg of all backbone atoms of the apo hER $\alpha$ LBD throughout 100 ns MD simulations for (a) <b>3ap</b> and <b>3ap_c</b> , (b) <b>4an</b> , <b>2an_c</b> and (c) <b>5ag</b> , <b>ag_c</b> . Figure was generated using xmgrace software	108
Figure 4.29	RMSF profiles of the hER $\alpha$ free and complex throughout simulations time for (a) <b>3ap</b> and <b>3ap_c</b> , (b) <b>4an</b> , <b>2an_c</b> and (c) <b>5ag</b> , <b>ag_c</b> . Figure was generated using xmgrace software	111
Figure 4.30	Overlay of snapshots of the conformational dynamics taken at different simulation times for the apo, antagonist and agonist hER $\alpha$ bound to <b>5c</b> (a) <b>3ap_c</b> , (b) <b>4an_c</b> and (c) <b>5ag_c</b> . Figure was generated using Chimera 1.11.2 software	113

Figure 4.31	The RMSDs of <b>5c</b> ligand in the binding pocket for apo (black), antagonist (red) and agonist (blue) throughout 100 ns MD simulations. Figure was generated using xmgrace software	114
Figure 4.32	(a) 2D and 3D structures of <b>5c</b> . The Ligand dynamics snapshots in the binding pocket taken at different simulation times for (b) <b>3ap_c</b> , (c) <b>4an_c</b> and (d) <b>5ag_c</b> systems. Figure was generated using Chimera 1.11.2 software	116
Figure 4.33	The percentage of occupancy of hydrogen bonds between amino acids residues in the three hER $\alpha$ - <b>5c</b> complexes (a) <b>3ap_c</b> , (b) <b>4an_c</b> and (c) <b>5ag_c</b>	119
Figure 4.34	Atoms involved in the hydrogen bonding for the apo, antagonist and agonist hER $\alpha$ bound to <b>5c</b> (a) <b>3ap_c</b> , (b) <b>4an_c</b> and (c) <b>5ag_c</b>	120
Figure 4.35	Benzophenone imine, <b>5c</b> , induce a disrupted conformation of the hER $\alpha$ ligand-binding domain. (A, B) Free agonist 1G50 hER $\alpha$ structure and antagonist 3ERT hER $\alpha$ LBD bound to the 4-OHT at the end of simulation, respectively. conformations show a $\sim 1$ Å difference in distance between helices 3 and 11. (C) structure of the antagonist 3ERT hER $\alpha$ in complex with compound <b>5c</b> shows a TAM-like binding orientation and increased H3–H11 distance compared to free agonist and 4-OHT complex. Figure was generated using PyMOL software	123
Figure 4.36	Amino acids contributions of apo hER $\alpha$ - <b>5c</b> complex, <b>3ap_c</b> , (a) The binding pose of apo hER $\alpha$ - <b>5c</b> in the binding site at 100 ns. (b) The mapping of energy contributions on the structure of hER $\alpha$ - <b>5c</b> ( <b>3ap_c</b> ). (c) Intermolecular ligand-receptor per-residue interaction spectrum of the <b>3ap_c</b> complex. Figure was generated using Chimera 1.11.2, VMD and xmgrace softwares	127
Figure 4.37	Amino acids contributions of the antagonist hER $\alpha$ - <b>5c</b> complex <b>4an_c</b> . (a) The binding pose of <b>5c</b> and antagonist hER $\alpha$ in the binding site at 100 ns. (b) The mapping of energy contribution on the structure of <b>4an_c</b> . (c) Intermolecular ligand-receptor per-residue interaction spectrum of the <b>4an_c</b> complex. Figure was generated using Chimera 1.11.2 , VMD and xmgrace softwares	128
Figure 4.38	Amino acids contributions of agonist hER $\alpha$ - <b>5c</b> complex <b>5ag_c</b> . (a) The binding pose of <b>5c</b> and agonist hER $\alpha$ in the binding site at 100 ns. (b) The mapping of energy contribution on the structure of <b>5ag_c</b> . (c) Intermolecular ligand-receptor per-residue interaction spectrum of the <b>5ag_c</b> complex. Figure was generated using Chimera 1.11.2, VMD and xmgrace softwares	

## LIST OF ABBREVIATIONS

AF-1	Activation Function 1
AF-2	Activation Function 2
Ala	Alanine
AMBER	Assisted Model Building and Energy Refinement
Arg	Arginine
Asp	Aspartic acid
BIs	Benzophenone Imines
BPs	Benzophenones
BZA	Bazedoxifene
CHD	Coronary Heart Disease
DBD	DNA Binding Domain
DES	Diethylstilbestrol
E1	Estrone
E3	Estriol
E2	17 $\beta$ -estradiol
ERs	Estrogen Receptors
EREs	Estrogen Response Elements
ER $\alpha$	Estrogen Receptor Alpha
ER $\beta$	Estrogen Receptor Beta
Phe	Phenylalanine
FTIR	Fourier Transform Infrared Spectroscopy
GEN	Genistein
GROMACS	Groningen Machine for Chemical Simulation

Glu	Glutamic acid
Gly	Glycine
H12	Helices 12
HDACi	Histone Deacetylase Inhibitors
His	Histidine
HSP 90	Heat-Shock Protein 90
Ile	Isoleucine
LBD	Ligand Binding Domain
Leu	Leucine
LFX	Lasofloxifene
Lys	Lysine
LJ	Lennard-Jones Repulsion/Dispersion Potential Energy
MD	Molecular Dynamics
Met	Methionine
MM-PBSA	Molecular Mechanics Poisson-Boltzmann Surface Area
NMR	Nuclear Magnetic Resonance
NR	Nuclear Receptor
NPT	Constant Number of Molecules, Pressure and Temperature
NVT	Constant Number of Molecules, Volume and Temperature
NVE	Constant Number of Molecules, Volume and Energy
4-OHT	4-hydroxytamoxifen
PBC	Periodic Boundary Conditions
PDB	Protein Data Bank
PR	Progesterone Receptor
PME	Particle Mesh Ewald

PM3	Parameterized Model Number 3
RAM	Random Access Memory
$R_g$	Radius of Gyration
RXR $\alpha$	Retinoic X Receptor Alpha
RMSD	Root Mean Square Deviation
RMSF	Root Mean Square Fluctuation
SASA	Solvent Accessible Surface Area
SERMs	Selective Estrogen Receptor Modulators
SERDs	Selective Estrogen Receptor Down Regulators
TAM	Tamoxifen
TLC	Thin Layer Chromatography
Trp	Tryptophan
Thr	Threonine
TIP3P	Transferable Intermolecular Potential with 3 Points
Val	Valine
vdW	van der Waals

## LIST OF SYMBOLS

$\Delta G_{binding}$	Total binding free energy
$\Delta G_{exp}$	Experimental total free energy
$\Delta G_{calc}$	Calculated total free energy
$\Delta G_{complex}$	Total free energy of the protein–ligand complex
$G_{solvation}$	Free energy of solvation
$G_{protein}$	Total free energy of the isolated protein
$G_{ligand}$	Total free energy of the isolated ligand
$E_{MM}$	Potential energy in vacuum
$E_{bonded}$	Bonded interactions
$E_{nonbonded}$	Nonbonded interactions
$E_{elec}$	Electrostatic interaction
$E_{vdW}$	van der Waals interaction
$\Delta S_{conf}$	Loss of conformational entropy upon binding to protein
$K_i$	Inhibition constants
$V$	Potential energy
$N_{tors}$	Number of active torsions
$F_i$	Force exerted on molecule $i$
$m_i$	Particle mass

$a_i$	Acceleration of molecule $i$
$\epsilon$	Depth of potential well
$\sigma$	Finite value of $r$
$m_i$	Mass of molecule $i$
$V_i$	Velocity of molecule $i$
$R$	Position
$T$	Temperature
$S$	Entropy
$\gamma$	Coefficient related to surface tension of the solvent
$u_{LJ}$	The Lennard-Jonnes potential
Nm	Nanometer
Ns	Nanosecond
$\mathbf{v}(t)$	Velocities Verlett algorithm
$r^2(t)$	Mean square displacement

# **REKABENTUK DAN KAJIAN PENGKOMPUTERAN PERENCAT KANSER PAYU DARA BENZOFENON DAN BENZOFENON IMINA BAHARU**

## **ABSTRAK**

Kaedah pengkomputeran melibatkan interaksi protein-ligan adalah suatu komponen penting dalam reka bentuk dadah dan penemuan dadah baharu. Kajian ini cuba untuk mereka bentuk dan mengkaji interaksi perencat reseptor estrogen manusia (hER $\alpha$ ) baharu untuk merawat sel kanser payu dara. Perencat cadangan direka melalui penggantian kumpulan berfungsi perancah estrogen triariletilena yang ditemui pada perencat hER $\alpha$  sintetik, 4-hidroksitamoxifen (4-OHT) dengan kumpulan berfungsi terbitan triarilimina bes Schiff. Selain itu, kajian ini bermatlamat untuk membangunkan sebatian dengan ekor perancah anti estrogen melalui kemasukan kefungsi rantai sampingan asid amino alanin ke dalam perancah triarilimina. Analisis biologi ujian hukum lima Lipinski menunjukkan perencat baharu yang direkabentuk mematuhi kriteria dadah berpotensi. Justeru, interaksi hER $\alpha$  dengan 16 ligan morfolin eter benzofenon (BPs) dan benzofenon imina (BIs) yang direka telah dikaji menggunakan kaedah pendokkan molekul, simulasi dinamik molekul dan pengiraan tenaga luas permukaan mekanik molekul Poisson-Boltzmann (MM-PBSA) untuk meramal mod pengikatan dan mengira tenaga bebas kompleks hER $\alpha$ . Keputusan kajian pendokkan molekul menggunakan Autodock 4.2.6 mendedahkan bahawa BIs yang baharu direka bentuk terikat pada poket terbuka hidrofobik hER $\alpha$  apo dan antagonis dengan afiniti yang lebih tinggi daripada estrogen semula jadi estradiol (E2) dan sintetik 4-hidroksitamoksifen (4-OHT) menyerupai tingkah laku 4-OHT. Tambahan lagi, gaya pendokkan BIs memaparkan mod interaksi tunggal dengan tapak terbuka hER $\alpha$  apo dan antagonis sementara BPs memaparkan

kelompok berbilang orientasi. Simulasi dinamik molekul telah dijalankan menggunakan GROMACS 5.0.7 dan menggunakan medan daya AMBER FF99SB-ILDN. Analisis keputusan simulasi dinamik molekul 100 ns daripada enam sistem berlainan bagi BI terbaik, **5c**, dengan hER $\alpha$  menunjukkan bahawa **5c** membentuk interaksi yang stabil dan kurang mengalami perubahan konformasi turun naik dalam reseptor hER $\alpha$  apo/antagonis terbuka berbanding agonis tertutup. Analisis seterusnya menunjukkan bahawa kebanyakan residu asid amino dalam kompleks hER $\alpha$ -**5c** agonis mengalami perubahan turun naik berbanding kompleks antagonis yang membentuk interaksi stabil. Selain itu, analisis penghunian ikatan hidrogen menunjukkan pembentukan ikatan hidrogen tertinggi di antara **5c** dan asid amino Glu353, His524 dan Thr347. Keputusan MM-PBSA mengesahkan kestabilan yang lebih tinggi bagi sistem hER $\alpha$ -**5c** apo/antagonis dan memperlihatkan bahawa interaksi hidrofobik merupakan penyumbang utama dalam pembentukan kompleks hER $\alpha$ .

# **COMPUTATIONAL DESIGN AND INVESTIGATION OF NEW BENZOPHENONES AND BENZOPHENONE IMINES INHIBITORS FOR BREAST CANCER**

## **ABSTRACT**

The computational methods of protein-ligand interactions are core components in drug design and modern drug discovery. This study attempted to design and investigate the interactions of new human estrogen receptor (hER $\alpha$ ) inhibitors to treat breast cancer cells using molecular modeling approach. The proposed inhibitors were designed by replacing the triarylethylene estrogenic scaffold found in the synthetic inhibitor 4-hydroxytamoxifen (4-OHT) with triarylimine Schiff bases. Besides, compounds with antiestrogen scaffolds tail through the incorporation of alanine amino acid side chain functionality into the triarylimine scaffolds were developed. Lipinski's rule of five revealed that the newly designed inhibitors conforms to the potential drug criteria. In light of these considerations, the interactions of hER $\alpha$  with 16 newly designed morpholine ether benzophenone (BPs) and benzophenone imines ligands (BIs) ligands were investigated using molecular docking, molecular dynamics simulations and molecular mechanics Poisson-Boltzmann surface area (MM-PBSA) energy calculations. Molecular docking study using Autodock 4.2.6 revealed that the newly designed BIs bind to the hydrophobic open pocket of the apo and antagonist hER $\alpha$  conformations with higher affinity compared to the natural and synthetic estrogen estradiol (E2) and 4-hydroxytamoxifen (4-OHT) and mimicked the behavior of the synthetic inhibitor, 4-OHT. Furthermore, docking poses of the BIs displayed single mode of interaction with the open binding site of apo and antagonist hER $\alpha$  forms while the BPs displayed multiple cluster orientations. Molecular dynamics simulations was conducted using GROMACS 5.0.7 with the AMBER FF99SB-ILDN

force field. The analysis of a 100 ns molecular dynamics simulations results on six different systems of the best docked BIs ligand, **5c**, with hER $\alpha$  demonstrated that **5c** forms stable interactions and undergoes less conformational fluctuations in the open apo/antagonist hER $\alpha$  receptors compared to the closed agonist binding site. Further analysis revealed that most of the amino acids residues in the agonist hER $\alpha$ -**5c** complex undergo fluctuation compared to the antagonist which form stable interaction. Besides, the analysis of hydrogen bonds occupancy reported the highest formation of hydrogen bonds between **5c** and amino acid residues Glu353, His524 as well as Thr347. The MM-PBSA results confirmed the higher stability of hER $\alpha$ -**5c** apo/antagonist systems and revealed that the hydrophobic interactions is the main contributor which stabilizes the formation of the receptor-inhibitor complexes.

# CHAPTER 1

## INTRODUCTION

### 1.1 Breast Cancer

Breast cancer is the most common cancer among females in the Asia-Pacific region, accounting for 18% of all cases in 2012, and was the fourth most common cause of deaths (Youlden et al., 2014). Although breast cancer incidence rates remain much higher in New Zealand and Australia regions, rapid rise in recent years were observed in several Asian countries, particularly Malaysia and Thailand. Incidence and mortality estimates for the year 2012 in Malaysia were 5,410 and 2,572 cases, respectively (Ghoncheh et al., 2016; Youlden et al., 2014).

A common treatment of hormone-sensitive breast cancer in the early-stage is surgery to remove the tumour followed by radiotherapy (Downey et al., 2007). Furthermore, chemotherapy or hormone therapy can be given to patient in order to remove or blocks the action of hormones such as estrogen and progesterone which are recognised as key molecular drivers in breast cancer (Blamey, 2003; Downey et al., 2007). In healthy women, estrogens are mainly produced in the ovaries and also in adipose tissue, breast, skin and bone (Nelson & Bulun, 2001). During the post-menopause period, breasts are the major source of estrogen production. Thus, the level of estrogens produced in the breast are comparable to that produced in the ovaries by premenopausal women (Blamey, 2003). Approximately 60% of pre-menopausal and 75% of post-menopausal cancer are estrogen dependent (Russo et al., 2003). The discovery of the link between breast cancer, estrogen, and estrogen receptors (ERs) has made a remarkable contribution to improve cancer treatment and reduce the mortality rate (Koř et al., 2001). Estrogen receptor positive i.e, ER+, in

breast cancer cells exert an estrogen promoted proliferation through ER-regulated gene transcription (Ebner et al., 2009). If the growth stimulated by estrogen can be blocked, then we may be able to control breast cancer (Riggs & Hartmann, 2003).

The hormone, estrogen (17 $\beta$ -estradiol, E2) has been identified as a key molecular stimulant in the development of ER positive breast cancer, which constitutes to around 70-80% of all breast cancers (Johnston & Dowsett, 2003). In premenopausal women, estrogens are produced primarily in the ovaries. However, the ovaries almost stop to secrete estrogen in postmenopausal women and the serum concentration of estrogen thus decreases dramatically (Pasqualini et al., 1996). Residual levels of estrogen are also commonly found circulating in the blood plasma and are around 20-fold higher in post-menopausal women compared to pre-menopausal women despite the loss of ovarian estrogen production (Larionov et al., 2003; Simpson & Dowsett, 2002). A cumulative exposure to estrogen does encourage the development of female reproductive cancers. Such examples include breast cancer and uterus cancer, which are associated with hormone replacement therapy, early menarche and late menopause (Feigelson & Henderson, 1996). The contribution of estrogens in various physiological and pathological pathways highly depends on their binding to estrogen receptors and activating transcription of estrogen responsive genes (Hortobagyi, 2012).

The x-ray crystal structure of ligands bound to the estrogen receptor provides experimental data to explain the ligand binding orientation, shape of the ligand binding pocket and explain the activity of synthetic ligands (Tanenbaum et al., 1998). Unfortunately, researchers do not always have the capability to synthesis and test all possible ligands with the estrogen receptor. So methods such as molecular modeling technique is used to help predict the size and shape of the ligand in the binding pocket, and the ligand binding orientation (Sliwoski et al., 2014). Computer-aided design is a useful method to rationalize the choice of suitable ligands in the context of known x-ray structure of the proteins (Sliwoski et al., 2014). AutoDock 4.2 software is a modeling program implementing a force field to calculate the binding energy of the ligand-receptor complex to predict the nature of the ligand orientation and the shape of the binding pocket (Morris et al., 2009). Moreover, using a molecular dynamics simulation approach, ligand-receptor complex interaction can be investigated and studied to gain a better understanding of the complex stability and this information can be used to design new inhibitors (Piana et al., 2011).

## **1.2 Problem Statement**

Despite the great advances in treatment provided by mammographic screening and enhanced hormone therapy, breast cancer remains one of the most pressing threats to women's health worldwide and has been the leading cause of death (Fontham et al., 2009). Though the use of antiestrogens in hormone therapy has proven invaluable in preventing the illness, breast cancer remains a persistent danger as the treatment method often experiences a high rate of acquired resistance and suffers from a variety of side-effects such as endometrial cancer, osteoporosis and the risk of coronary heart disease (CHD) (Ring & Dowsett, 2004). The selective estrogen receptor modulator (SERM) tamoxifen is a front-line treatment for the disease, but it suffers from a high

rate of resistance and an increased risk of endometrial cancer. As such, novel small molecules inhibitor with the ability to overcome antiestrogen resistance while limiting the adverse side effects are valuable pharmaceutical targets. This thesis describes new approaches to design inhibitors through the incorporation of benzophenone and imine derivatives inhibitors functionality into the antiestrogen scaffolds to generate functional hybrid molecules.

### **1.3 Aims of the Study**

The objectives of this research are:

1. To design new benzophenones (BPs) and benzophenone imines (BIs) inhibitors for human estrogen receptor hER $\alpha$  to treat breast cancer.
2. To investigate the structural and dynamical features of the newly designed BPs and BIs during the interactions with hER $\alpha$  using molecular docking and molecular dynamics simulation.
3. To analyze the stability and structural change of the newly designed benzophenone and benzophenone imines ligands following the complexation with three hER $\alpha$  forms i.e agonist, antagonist and apo conformations, in order to provide new information that might be useful to develop new inhibitors with improved anti-estrogenic property to treat breast cancer cells.

## CHAPTER 2

### LITERATURE REVIEW

#### 2.1 The Estrogen Receptor: Structures and the Mechanism of Action

##### 2.1.1 Estrogen and the Estrogen Receptor (ER)

Estrogens are hormones that are important for sexual and reproductive development, mainly in women. They are produced primarily in the part with grape-sized glands located in the uterus and are part of the endocrine system called ovaries (Burger, 2002). The predominant and most potent of these hormones is 17 $\beta$ -estradiol (E2) which is essential for the female reproductive system (Fogle et al., 2007). On the other hand, estrogen are involved in the development and progression of breast tumors due to its amplification of malignant cell growth and to the high risk of DNA replication errors associated with its growth-promoting abilities (Burger, 2002).

Estrogens in women are steroid hormones, which are biosynthesized from cholesterol via multiple enzymatic steps as shown in Figure 2.1 (Larionov et al., 2003). Aromatase is one of the most important enzymes catalyzing the biotransformation to finally produce estrogens, E2 which is the most potent female hormone (Johnston & Dowsett, 2003). The estrogen receptor belongs to the nuclear receptor (NR) superfamily and exists as two major subtypes: estrogen receptor alpha (ER $\alpha$ ) and beta (ER $\beta$ ) (Moore et al., 2006). Both are expressed in breast, bone, cardiovascular and brain tissue, but ER $\alpha$  is dominantly expressed receptor in uterine and liver cells whereas ER $\beta$  is the primary isoform in the gastrointestinal tract and colon (Pearce & Jordan, 2004).

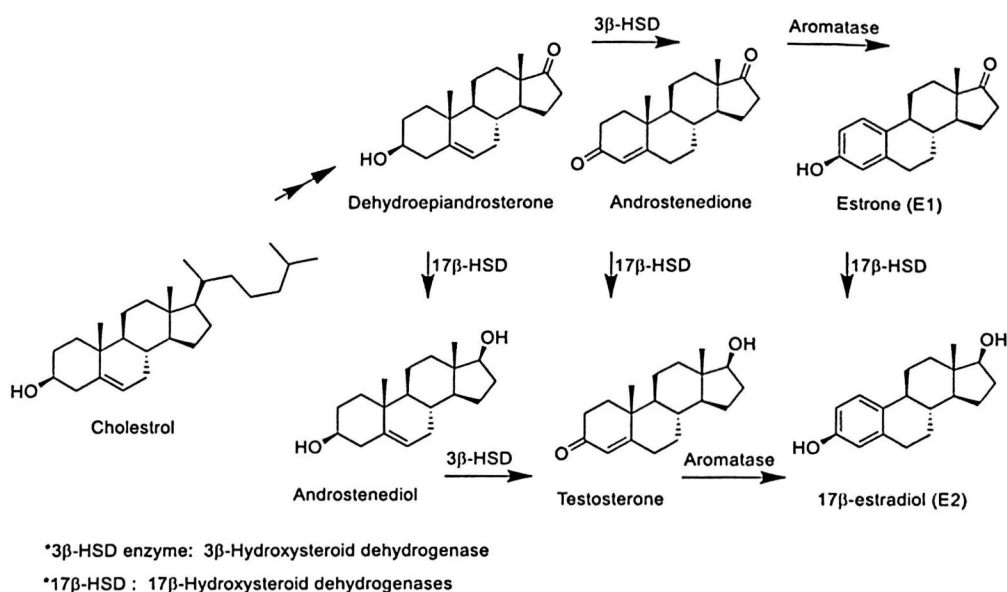


*Figure 2.1.* The major biosynthetic paths of endogenous Estrone (E1) and 17β-estradiol (E2) (Larionov et al., 2003). Figure was generated using ChemDraw16 software.

ER was first identified in the 1960s when the development of radiolabelled hormones made it possible to explain the binding of estrogen to its receptor (Jensen et al., 1968). ER is a nuclear transcription factor and normally involved in pathways controlling cell proliferation (Beato & Klug, 2000). Approximately 80% of all breast cancers have ER+ tumor cells (Anderson et al., 2002). The role of ER $\alpha$ , and its ligands in breast carcinogenesis has been recognized for some time (Yager & Davidson, 2006). Estrogens play a critical role in sexual development, reproduction and many physiological processes. Furthermore, ER plays a vital role in the development, progression, treatment and outcome of breast cancer (Koř et al., 2001).

In the classic pathway, binding of estrogen to the estrogen receptors (hER  $\alpha$  and  $\beta$ ) induces a dynamic conformational change that leads to ER dimerization and association with co-regulatory proteins with the subsequent transcriptional activation of estrogen-responsive genes (Zhou & Davidson, 2006). Anti-estrogens such as

selective estrogen receptor modulators (SERMs) act as competitive blockers of estrogen-ER binding, and have been successfully used in the treatment of ER $\alpha$  positive breast cancer (Riggs & Hartmann, 2003). In the adjuvant setting, tamoxifen reduces the rate of disease recurrence and has led to a significant reduction in breast cancer mortality in the past few decades (Rao & Cobleigh, 2012).

ERs are composed of six function domains designated A-F, Figure 2.2, referred to as the N-terminal A/B domain, the DNA binding domain (C), the hinge domain (D), the ligand binding domain (LBD, E), and the C-terminal F domain (Bourguet et al., 2000). The final C-terminal E/F domain encodes the LBD, which is consists of 12  $\alpha$ -helices (H1-12) that form a hydrophobic binding pocket responsible for estrogen and antiestrogen binding (Shiau et al., 1998). This domain also contains a second ligand-dependant activation factor, AF2, which activates ER in response to E2 or synthetic agonists. Due to the implication of controlling ER activity through its modulation, the LBD is important for the development of synthetic agonists and antagonists (Aranda & Pascual, 2001).

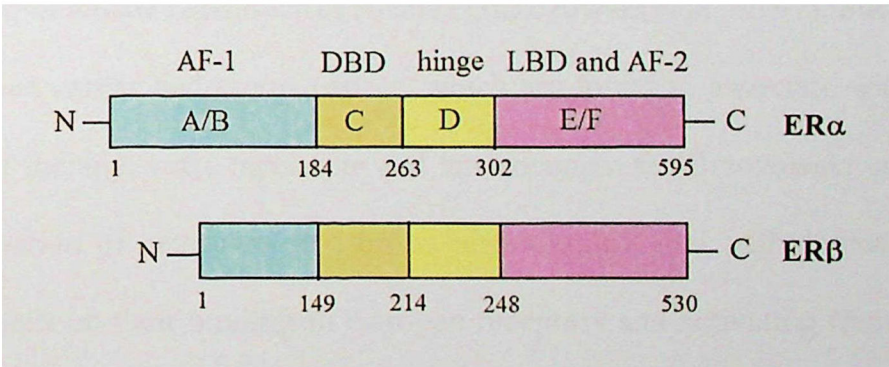


*Figure 2.2.* The human estrogen receptor  $\alpha$  and  $\beta$  (hER $\alpha$  and hER $\beta$ ) where A/B is the N-terminal domain, C is the DNA binding domain, D is the hinge domain and E/F C-terminal domain.

Transcriptional activity differs when different ligands bind to the NR. Meanwhile, the position of the C-terminal helix, helix12 (H12), also differs when different ligands bind to the NR (Bourguet et al., 2000). It is reported that the transcriptional activity correlates with the position of the H12 (Aranda & Pascual, 2001). The position of H12 is far from the ligand binding pocket in the apo state (Tanenbaum et al., 1998), while a large structural change occurs and the H12 is situated near the ligand binding pocket when the ligand is bound. Such positions of the H12 are depend on the type of ligand. When the agonist binds to the NR, the H12 is repositioned to cap the ligand binding site, allowing the co-activator protein to bind and the transcription to take place (Wärnmark et al., 2002). On the other hand, the H12 lies over the coactivator groove when the antagonist binds to the NR, thus preventing dimerization and transcription from occurring (Shiau et al., 1998). All these conformations share a certain similarity in the binding site region, but a major differences in the H12 position (Egner et al., 2001).

A cumulative exposure to estrogen have been reported to encourage the development of female reproductive cancers (Brzozowski et al., 1997). Such examples include breast cancer and uterus cancer, which are found to associate with hormone replacement therapy, early menarche and late menopause (Brzozowski et al., 1997). The contribution of estrogens in various physiological and pathological pathways highly depends on their binding to estrogen receptors and activating transcription of estrogen responsive genes (Castelo-Branco et al., 2000).

E2 is planar, non-polar, hydrophobic and contains two hydroxyl groups, a phenolic hydroxyl group on the A-ring and a 17 $\beta$ -hydroxyl group on the D-ring. Upon binding to the ligand binding domain (LBD) of human estrogen receptor (hER $\alpha$ )

estradiol rests in a binding cavity within the hydrophobic core of the LBD formed by helices H3, H6, H8, H11 and H12 (Anstead et al., 1997).

The substrate, E2, occupies a series of specific hydrogen bonds by two hydroxyl groups. The phenolic hydroxyl from the A ring forms direct hydrogen bonds with the carboxylate of a glutamic acid residue in H3 (Glu353), the arginine residue in H6 (Arg394). On the other hand, the 17 $\beta$ -hydroxyl group at the D ring forms hydrogen bonding with a single histidine residue in H11 (His524), Figure 2.3. The hydrophobic core of E2 also plays a role in binding with hydrophobic residues of ER-LBD, which forms close contacts with alanine and phenylalanine that serve to orient the ligand (Anstead et al., 1997). The results of the hydrophobic and polar binding mode of E2 is the folding of H12 across H3 and H11, leading to the agonist conformation of the LBD and enhancing gene transcription (Brzozowski et al., 1997).

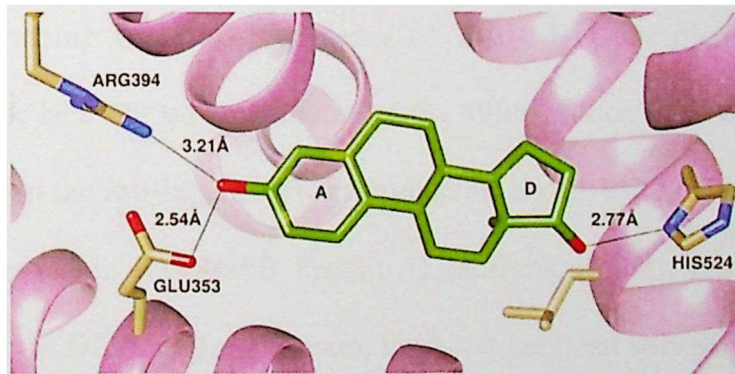


*Figure 2.3.* Binding mode of 17 $\beta$ -estradiol in ER $\alpha$  (PDB:1G50) (Brzozowski et al., 1997). Figure was generated using Chimera 1.11.2 software.

The human ER has a typical structure that is shared by all the members of the steroid receptor family (Moore et al., 2006). The amino acid sequence of human ER is composed of six function domains, the N-terminal receptor A/B domain which contains hormone-independent activation function 1 (AF-1), allowing the receptor to have basic transcription activity in the absence of ligand. The middle C domain

contains the DNA binding domain (DBD), which is responsible for ER binding to estrogen response elements (EREs) on the DNA with two zinc finger motifs (Beato, 1989).

The D domain is a small hinge region between the DNA binding, which is implicated in co-regulatory protein binding. The carboxy-terminal domains E and F contain the ligand-binding domain (LBD) and contains another activation domain (AF-2), which induces in modulating the agonist activity of non-steroidal inhibitors, as well as co-regulator binding sites (Montano et al., 1995). The LBD itself involves the ligand-dependent transcription activation functions AF-2 and AF-2a (Norris et al., 1997), heat-shock protein 90 (HSP 90) binding region (Chambraud et al., 1990), a nuclear localization signal (Picard & Yamamoto, 1987) and another dimerization domain (Peters & Khan, 1999).

Crystallographic structures for many of ER $\alpha$ -LBD complexes were initially determined in the late 1990s (Tanenbaum et al., 1998). Since the isolation of LBD is easier compared to the full-length estrogen receptor, about 100 LBD structures of ERs have been deposited in the RCSB Protein Data Bank (PDB). However, the other domains, except the DNA binding domain, have not yet been solved, and the complete structure of the five ER domains is still lacking (Tanenbaum et al., 1998).

The LBD crystal structure analysis revealed 12  $\alpha$ -helices (H1-12), five of which (H 3, 6, 8, 11 and 12) form a hydrophobic ligand-binding pocket responsible for estrogen and antiestrogen binding (Egner et al., 2001). The crystallographic structures of the ligand-ER $\alpha$  LBD complexes are generally classified as agonist and antagonist conformations based on the position of the C-terminal H12, Figure 2.4. When agonists such as estradiol bind to ER (Figure 2.4a) the ligand is trapped within a hydrophobic

binding cavity formed by helices H3 (blue), H6 (grey) and H11 (green) (Pike et al., 1999). This allows the inner hydrophobic surface of H12 (red) to fold across H3 and H11 and cap the entrance of the cavity. Conversely, antagonists such as the synthetic antiestrogen 4-hydroxytamoxifen (4-OHT) have polar or steric bulky side-chains and occupy the same binding cavity as agonists do, but forces H12 to move towards the open/antagonist conformation. This allows the H12 (red) to overlap the H3 (blue) and H5 (orange) region (Figure 2.4b) and occupies the surface area where the co-activator protein should bind (Pike et al., 1999).

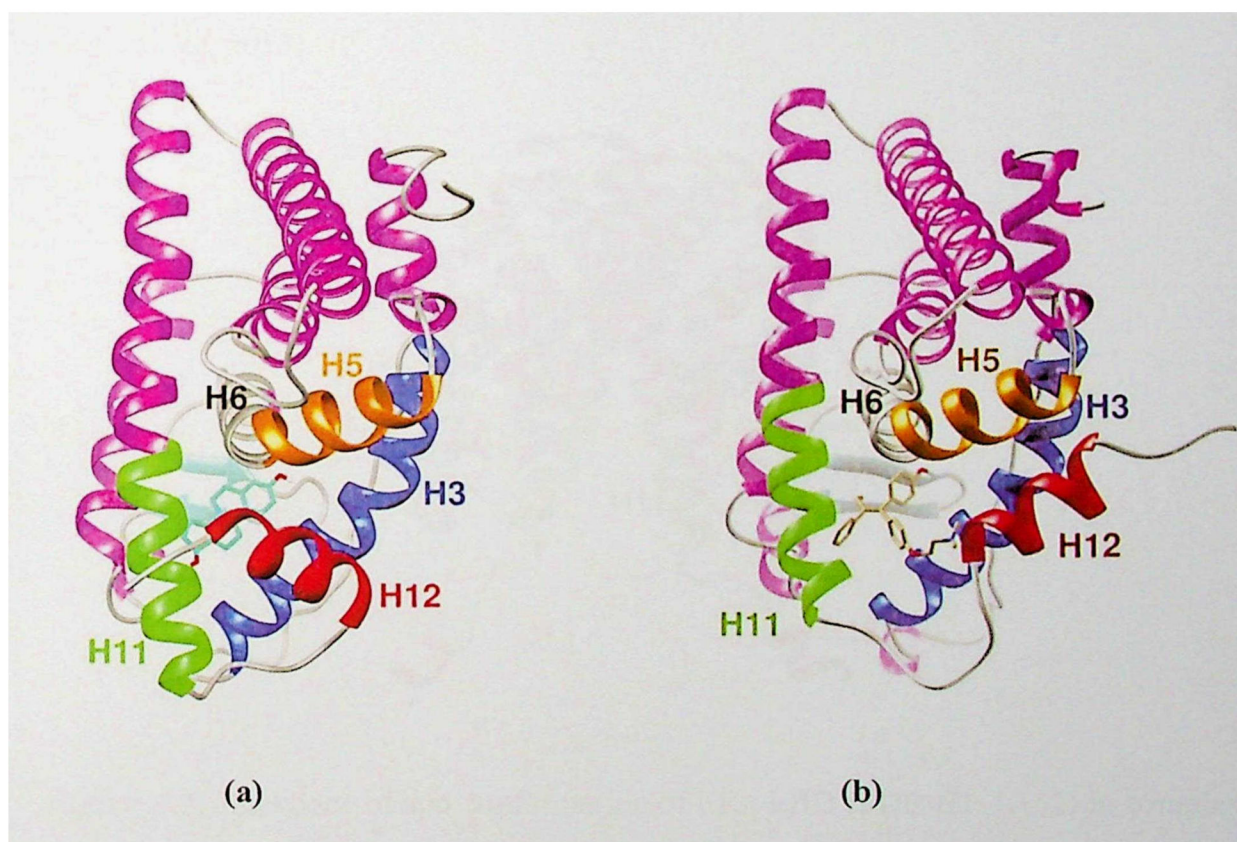


*Figure 2.4. (a) Backbone of agonist conformation of ER $\alpha$  LBD (PDB: 1G50) in complex with estradiol E2 (cyan stick). (b) Antagonist conformation of ER $\alpha$  LBD (PDB: 3ERT) in complex with 4-OHT (grey stick). Important helices are highlighted: H3 (blue), H5 (orange), H6 (grey), H11 (green) and H12 (red). Figure was generated using Chimera 1.11.2 software.*

The extended apo conformation of NR LBDs was first described in retinoic X receptor- $\alpha$  (RXR $\alpha$ ) (Bourguet et al., 1995), where H12 is extended away from the surface of the LBD core and does not have any hydrophobic interactions with the LBD. Similarly, the apo-form human estrogen receptor hER $\alpha$  PDB ID 1A52, Figure 2.5, also employs such an extended conformation (Tanenbaum et al., 1998). This shows that H12 is flexible and when comparing this form to known apo conformations of other NRs, the similarity is very obvious (Bourguet et al., 1995; Renaud et al., 1995). Initially, human estrogen receptor hER $\alpha$ -LBD with the PDB ID: 1A52 is commonly believed to serve as the best available conformation of an apo form (Batista & Martínez, 2013).

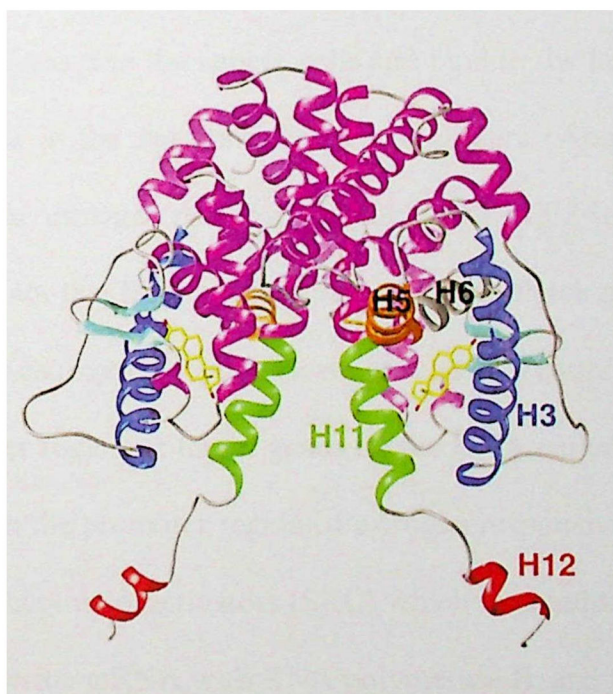


*Figure 2.5.* Backbone of apo conformation of ER $\alpha$  LBD (PDB ID: 1A52) in complex with estradiol (yellow). Figure was generated using Chimera 1.11.2 software.

In the apo conformation, H12 is extended away from the protein and is assumed to be fully solvated in the monomer. Crystal structure used to model the apo conformation reveals H12 is interacting with the other monomer of an LBD dimer (Tanenbaum et al., 1998). This cross-monomer interaction is an artifact of the crystal

structure. As pointed out by the authors, H11 and H12 in two adjacent monomers were synthetically linked with a disulfide bond. This forces H12 of one of the monomer to interact with the LBD of the other monomer.

### **2.1.2 The Mechanism of Action of the Estrogen Receptor**

Among the steroid receptors, estrogen receptor (ER) and the ER-regulated progesterone receptor (PR) are high in premalignant and malignant breast lesions as opposed to normal tissue (Aranda & Pascual, 2001). As a result, inhibition of the ER has become one of the major strategies for the prevention and treatment of breast cancer (Brzozowski et al., 1997).

Estrogen diffuses into the cancer cells and bind to the human estrogen receptor from blood plasma in the hormone-dependent cancers (Aranda & Pascual, 2001). Upon binding to the estrogen receptor, agonists such as E2 induce a conformational change in the receptor that leads to dissociation of heat-shock protein 90 (HSP 90) and dimerization of the estrogen receptor (Heery et al., 1997) as shown in Figure 2.6. Then, it binds to promoter region of target genes on the DNA called the estrogen response elements (EREs) in the promoter region of estrogen responsive genes. The ER dimer can bind steroid receptor co-activators (SRC) which then induce cellular transcription machinery to transcribe mRNA with RNA polymerase II, and the mRNA is translated into cellular proteins (Batista & Martínez, 2013).

Antagonist such as tamoxifen (commercial name Nolvadex) and raloxifene (Evista) are examples of selective estrogen receptor modulators (SERMs), that can deactivate the estrogen signalling pathway by competitive binding to ER, causing a conformational change to the subsequently formed ER dimer involving the shift of H12 into an adjacent coactivator site (AF2), thus blocking the binding of the

co-activator, which significantly reduces the level of estrogen-regulated gene transcription (Saha Roy & Vadlamudi, 2012).

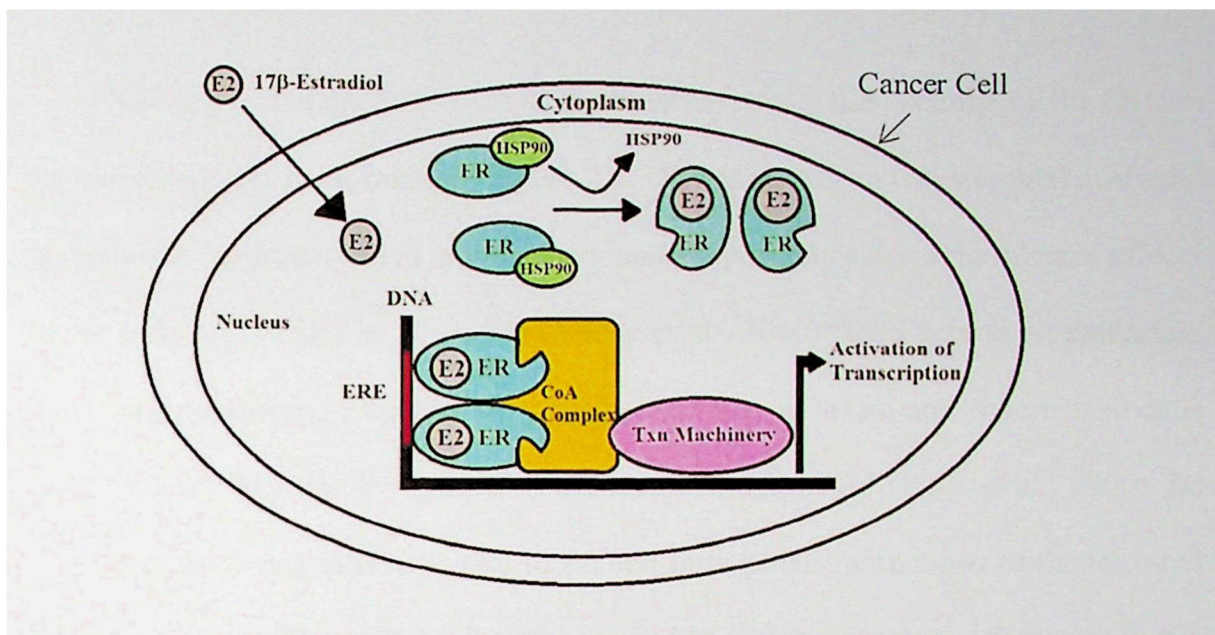


*Figure 2.6.* Mechanism of action of estrogen dependant gene transcription in cancer cell (Batista & Martínez, 2013).

The activation functions AF-1 and AF-2 mediate transcriptional activation of ER-regulated genes, which can function either independently or synergistically. Both of these domains have been shown to interact with distinct components of the basal transcription machinery, to mediate cell context-specific agonist and antagonist activities of antiestrogens, and to bind steroid receptor co-regulatory proteins (Yue et al., 2013). Therefore, cell-specific activity of AF-1 and AF-2 depends on the relative availability of co-regulatory proteins, the binding of which could either facilitate or disrupt the interaction of ER AF-1 and AF-2 with the basal transcription machinery leading to a regulated transcription of specific target genes. This transcription is implicated in the majority of breast tumour growth. Thus, methods for modulating or inhibiting ER activity through this pathway are central to breast cancer treatment (Deroo & Korach, 2006; Yue et al., 2013).

## 2.2 Agonists and Antagonists of the Estrogen Receptor

### 2.2.1 Full and Partial Agonists

Full and partial agonists such as diethylstilbestrol (DES) stabilize ER $\alpha$  LBD in the closed/agonist conformation, Figure 2.7. DES is a well-known steroidal synthetic agonists that has been used in pregnant women and possibly caused the adverse effects on the offspring (Giusti et al., 1995; O'reilly et al., 2010). DES acts as an extremely potent estrogen receptor agonist showing high activity in breast and endometrial cells and its affinity for ER $\alpha$  is reported to exceed even that of E2 (Blair et al., 2000). Its binding mode is very similar to that of E2 and form polar interactions of the terminal hydroxyl groups with Arg394, Glu353 and His524 which dictate its orientation in the binding pocket (Shiau et al., 1998). The two ethyl groups of DES is locate perpendicularly to the plane of the phenols to fit in hydrophobic the cavities within the pocket, where they form hydrophobic interactions with leucine and phenylalanine residues in the hER $\alpha$  LBD. In contrast, these cavities are unoccupied in the E2-bound complex where they are located over the planar ring area (Shiau et al., 1998). This behaviour suggests that the planar nature of estradiol is not necessary for potent ER affinity (Shiau et al., 1998).



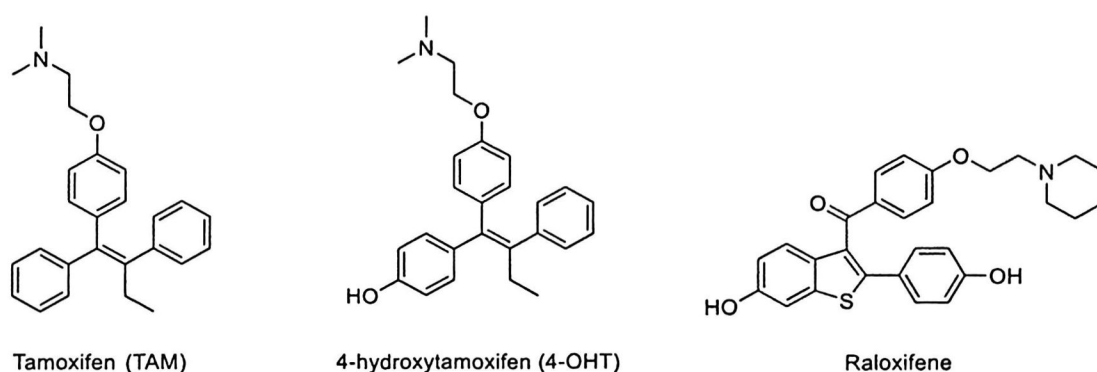
*Figure 2.7.* Structures of selected full and partial agonists ligands against ER $\alpha$  LBD.

Figure was generated using ChemDraw 16 software.

The bioactivity profiles of partial agonists are much more complicated due to the mixed agonist/antagonist properties. The soy phytoestrogen genistein (GEN), Figure 2.6, is a well-known partial agonist. The consumption of soy food has been suggested to reduce the risk of developing breast cancer (Warri et al., 2008). Although, GEN has also been found to stimulate breast cancer cell growth in some studies (Ju et al., 2006; Warri et al., 2008).

### 2.2.2 Partial Antagonist as Selective Estrogen Receptor Modulators (SERMs)

In contrast to full and partial agonists, partial antagonists stabilize ER $\alpha$  LBD in the open/antagonist conformation (Jordan, 2003a). Selective estrogen receptor modulators (SERMs) act as antagonists in some tissues but have agonistic properties in others such as tamoxifen (TAM), 4-hydroxytamoxifen (4-OHT) and raloxifene, Figure 2.8. The partial antagonist SERMs are effective small-molecule inhibitors in breast cancer tissue and have shown great success in endocrine therapy (Maximov et al., 2013).



*Figure 2.8.* Structures of selected ER $\alpha$  partial antagonists as selective estrogen receptor modulators (SERMs). Figure was generated using ChemDraw 16 software.

Tamoxifen (TAM) is used as a front-line endocrine therapy for breast cancer in pre-menopausal and post-menopausal women for the last 40 years. Besides, it is also used in the treatment of male breast cancer (Park & Jordan, 2002). The binding mode of 4-OHT in the binding site of ER $\alpha$  occupies the same hydrophobic binding pocket as E2, involving helices H3, H6, H8 and H11, Figure 2.9. Similar to the A-ring of E2, the phenolic hydroxyl group of OHT interacts with Glu353 and Arg394, (Shiau et al., 1998). The side-chain of 4-OHT, dimethylaminoethoxy group, lies through a narrow channel between H3 and H11, and the tertiary amine of the chain is placed near a surface aspartate residue, Asp351, (Saha Roy & Vadlamudi, 2012), Figure 2.9. This strong interactions prevent the hydrophobic inner surface of H12 from entering the region and folding over the binding pocket, thereby disrupting the coactivator surface and forcing the H12 orientation towards an open/antagonist conformation. For this reason, majority of SERMs possess an alkylaminoethoxy side-chain that contributes to blocking transcription of estrogen-dependant genes in breast tissue (Jordan, 2003b).

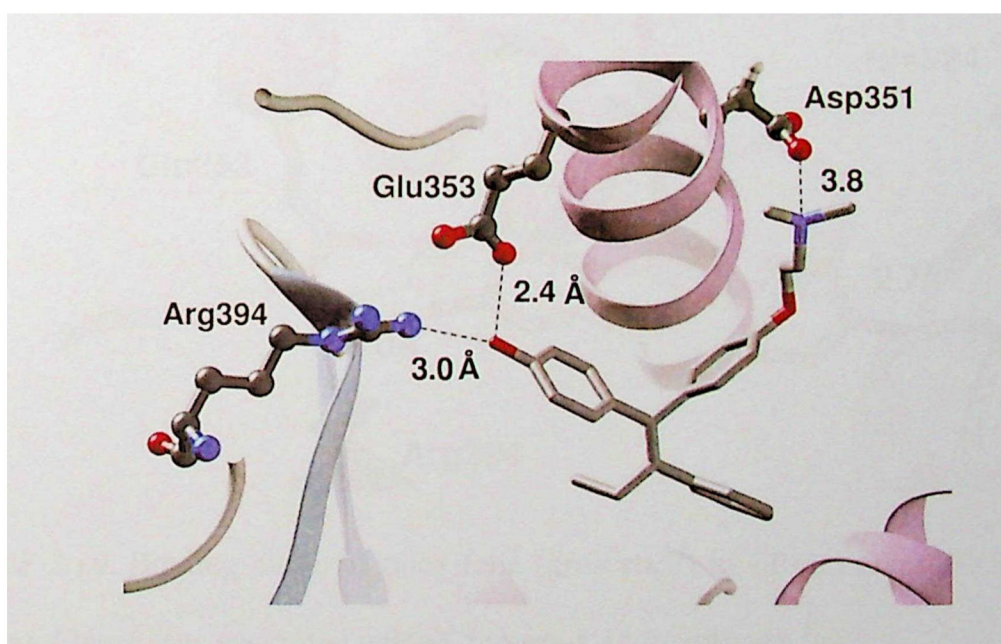


*Figure 2.9.* Binding mode of 4-hydroxytamoxifen 4-OHT in ER $\alpha$ , PDB: 3ERT (Park & Jordan, 2002). Figure was generated using Chimera 1.11.2 software.

The binding mode of raloxifene, Figure 2.10, in hER $\alpha$  is similar to that of tamoxifen in which its first phenolic hydroxyl group is bind to hER $\alpha$  through hydrogen bonds with Arg394 and Glu353 (Lewis & Jordan, 2005). As the benzothiophene SERM possesses a second phenolic hydroxyl on the other side, it forms a second hydrogen bond with His524 in the ER $\alpha$ -LBD (Jordan, 2003a). The interactions of side-chain terminal in raloxifene with Asp351 differ from tamoxifen side-chain interaction as the alkylaminoethoxy side-chain is significantly stronger in raloxifene compared to 4-OHT. The side-chain adopts a position much closer to the Asp351 residue, 2.7 Å compared to 3.8 Å and this contributes to an improved shielding of Asp351 from H12 binding and an increased antagonistic effect (Lewis & Jordan, 2005).

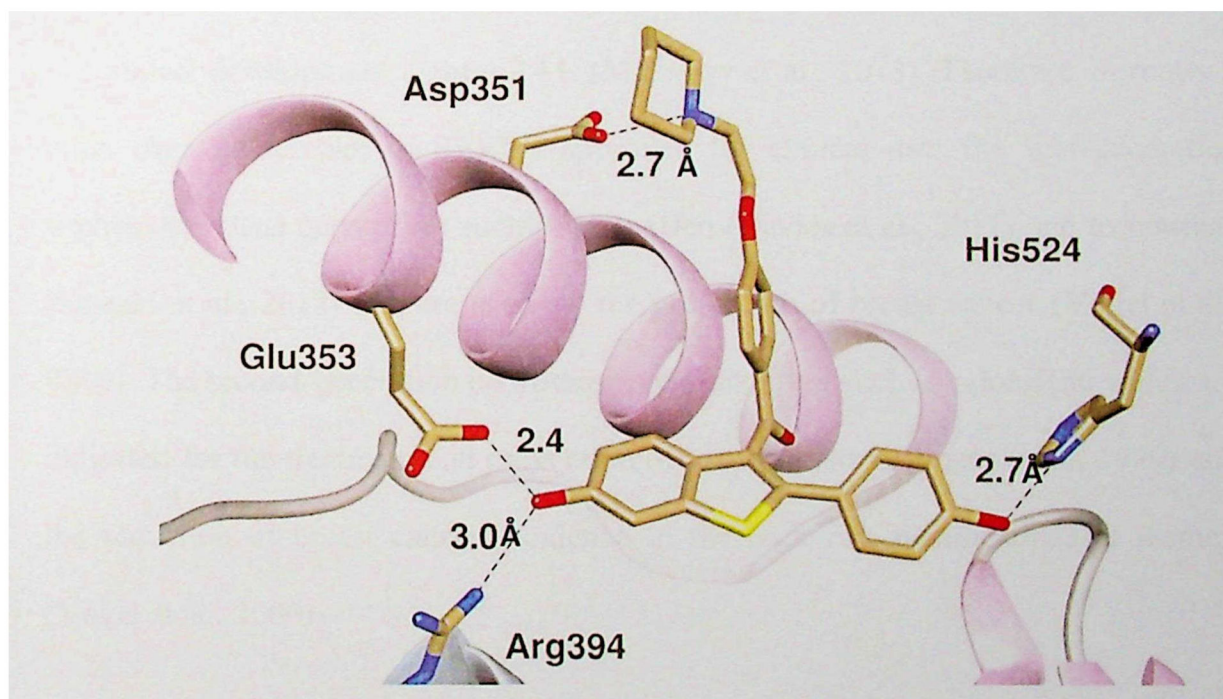
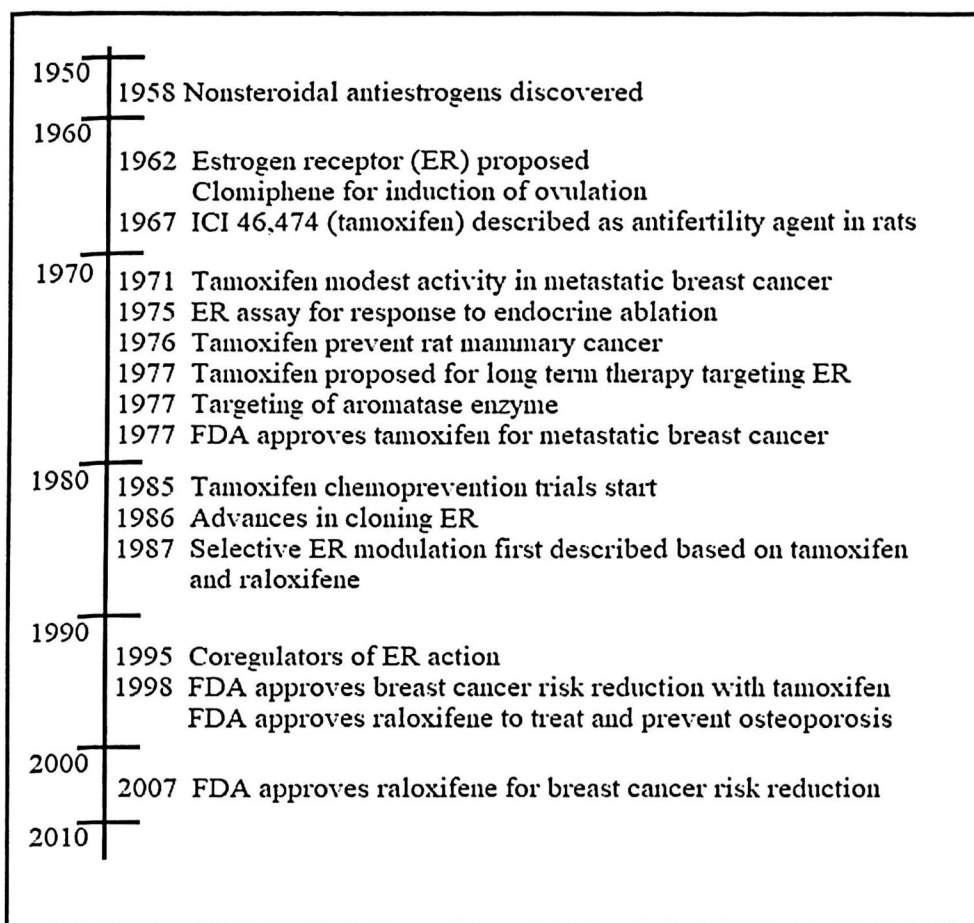


*Figure 2.10.* Binding mode of raloxifene (grey stick) in ER $\alpha$ , PDB: 1ERR (Jordan, 2003a). Figure was generated using Chimera 1.11.2 software.

The interactions between SERM's antiestrogenic side chain and amino acid Asp351 is important in disruption AF-2. It forces H12 to move away from the ligand-binding pocket thereby preventing coactivators from binding to the SERM-ER $\alpha$  complex (Jensen et al., 1968; Jordan, 2003b).

The effects of raloxifene side-chain and Asp351 amino acid interactions on the enhanced antagonistic properties was further demonstrated by amino acid substitution experiments. Mutation of Asp351 to glutamate results in an increased distance between the piperidine nitrogen and the protein residue and results in a subsequent increase in agonist effect (Liu et al., 2002).

In the latter half of the 20th century, the discovery and investigation of nonsteroidal antiestrogens by the pharmaceutical industry was a promising findings for clinical development, Figure 2.11, (Maximov et al., 2013). There are currently 2 main chemical classes of SERMs approved for clinical use: the first-generation triphenylethylene derivatives such as tamoxifen (Davies et al., 2011) and toremifene (Sawaki et al., 2012) that are used for the prevention of breast cancer (Vogel et al., 2010). The second-generation benzothiopene derivatives such as raloxifene which are indicated for the treatment and prevention of osteoporosis (Ettinger et al., 1999) and the reduction of breast cancer incidence in the high risk postmenopausal women (Vogel et al., 2006).

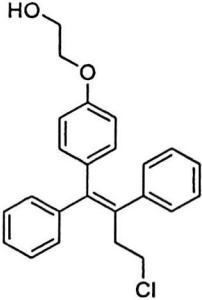
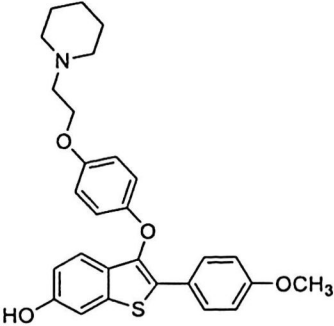
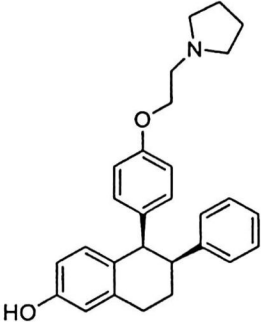
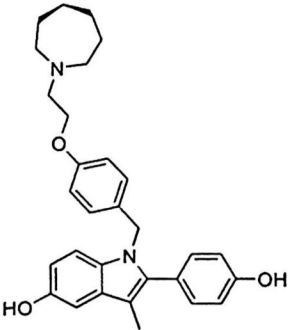


*Figure 2.11.* Timeline of the major estrogen, antiestrogens and SERMs for the treatment and prevention of breast cancer and osteoporosis (Maximov et al., 2013).

Raloxifene is an ER agonist in bone and cardiovascular system, but in breast tissue and endometrium it acts as an ER antagonist (Morello et al., 2003). The advantage of raloxifene over the triphenylethylene tamoxifen is it reduces effect on the uterus. The flexible hinge group, as well as the antiestrogenic phenyl 4-piperidinoethoxy side chain, are important for minimizing the uterine effects. Because of its flexibility, the side chain can obtain an orthogonal position relative to the core of raloxifene (Morello et al., 2003), so that the amine side chain of raloxifens is 1 Å closer than tamoxifen to Asp351 in hER $\alpha$ 's LBD (Lewis & Jordan, 2005). The discovery that tamoxifen had a breast cancer preventive effect but significantly increased the risk of endometrial cancer results in the search for better SERMs.

Third-generation SERMs such as ospemifene, arzoxifene, lasofoxifene (LFX) and bazedoxifene (BZA) have been used for the treatment of cancer (Table 2.1) but only LFX and BZA are approved by EU (Maximov et al., 2013).

Table 2.1: Details of new SERMs (Maximov et al., 2013).

Drug Name	Category	Chemical Structure	Effects
Ospemifene	Tamoxifen like		-Vaginal atrophy treatment. -Osteoporosis treatment. -Breast cancer prevention.
Arzoxifene LY353381	Raloxifene like		-Breast cancer treatment.
Lasofoxifene CP-336156- Fablyn	Raloxifene like		-Osteoporosis treatment. -prevention Vaginal atrophy. -Breast cancer treatment. -prevention heart disease.
Bazedoxifene TSE-424 WAY140424	Raloxifene like		-Osteoporosis treatment. -Breast cancer prevention.

### 2.2.3 Full Antagonist

The first pure antagonist ICI-164,384 was discovered by Wakeling et al., (1991). This compound is a 7 $\alpha$ -alkylamine derivative of 17 $\beta$ -estradiol with a 16 atom carbon chain in the 7 $\alpha$  position, Figure 2.11. This is then followed by a second, more potent alkylsulphinyll analogue ICI-182,780, also known as fulvestrant, Figure 2.12, (Wakeling et al., 1991). Fulvestrant is clinically available under the trade name Faslodex. It is used for the treatment of metastatic breast cancer in postmenopausal women following loss of response to tamoxifen therapy. Both compounds are 7 $\alpha$ -substituted structural derivatives of E2 with extended aliphatic side-chains (Bowler et al., 1989).

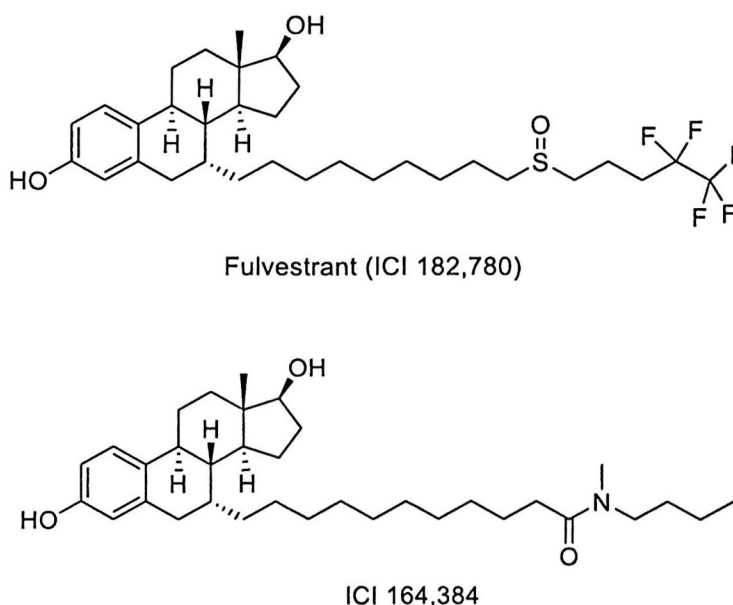


Figure 2.12. Structures of selected ER $\alpha$  pure antagonists (Wakeling et al., 1991).

Figure was generated using ChemDraw 16 software.

Fulvestrant is a selective estrogen receptor down-regulators (SERDs), an inhibitor that binds to the ER $\alpha$  and causes protein degradation. It is used to treat estrogen receptor-sensitive breast cancer, along with older classes of drugs like SERMs and aromatase inhibitors (Lee et al., 2017). It works by binding to the

estrogen receptor and making it more hydrophobic. This makes the receptor unstable and misfold, which in turn leads to normal processes inside the cell to degrade it. Faslodex was the first SERD to be approved in the US in 2002 and Europe in 2004 (Lee et al., 2017).

Fulvestrant possesses bulky hydrophobic alkyl-sulfinyl side chain located in the narrow channel between H3 and H11 and its terminus extended across the surface of AF2 region. This prevents H12 to move towards the pocket entrance and entire AF2 region altogether, resulting in a complete dissociation of the highly mobile H12 from the LBD which in turn leads to unstable and unfold receptor (Pike et al., 2001).

The hydrogen bonding interactions between LBD residues and pure antagonists occupies the same interaction as E2, as evidenced by the crystal structure of ICI 164,384 in ER $\beta$ , Figure 2.13. The A-ring phenol interacts with Glu260 and Arg301, whereas the 17 $\beta$  hydroxyl maintains an interaction with His430. However, ICI 164,384 is flipped 180° along its longest axis compared to E2 in order to adjust its bulky side-chain in the narrow channel between H3 and H11 (Pike et al., 2001).

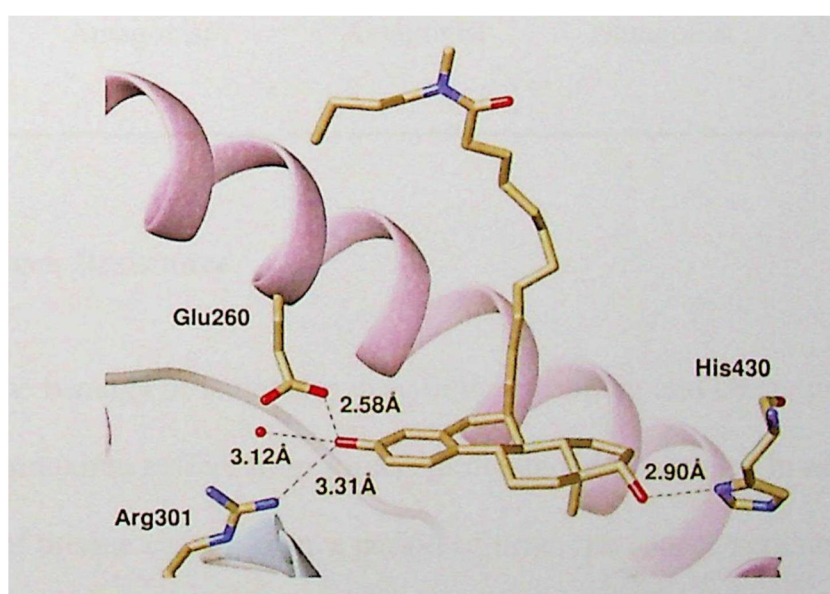


*Figure 2.13.* Binding mode of ICI 164,384 (grey stick) in ER $\beta$ , PDB: 1HJ1 (Pike et al., 2001). Figure was generated using Chimera 1.11.2 software.

Fulvestrant has been found to alter the antagonistic behaviour of full antiestrogens in comparison to the previously described SERMs. With complete disruption of the AF2 domain and deactivation of the AF1 domain, fulvestrant possess no agonistic behaviour in any tissue compared to SERMs (Bryant & Dere, 1998). Table 2.2 summarizes the effect of various ER $\alpha$  ligands, 17 $\beta$ -estradiol, two SERMs and two pure antiestrogens on some important tissues based on preclinical studies by Bryant & Dere, (1998).

Table 2.2: Estrogen behavior of various ligands in different tissues based on preclinical studies (Bryant & Dere, 1998).

Compound	Effects	Uterus Metabolism	Bone	Cholestrol
17 $\beta$ -estradiol	Agonist	Agonist	Agonist	Agonist
Tamoxifen	Antagonist	Partial Agonist	Agonist	Agonist
Raloxifene	Antagonist	Antagonist	Agonist	Agonist
ICI-164,384	Antagonist	Antagonist	Antagonist	Antagonist
Fulvestrant				

### 2.3 Antiestrogen Resistance

Despite the benefits of tamoxifen drug in the treatment and chemoprevention of breast cancer, tamoxifen suffers from some significant shortcomings. In addition to an increased risk of uterine cancer, over a period of time, the cancer patients eventually develop resistance to tamoxifen (Ali et al., 2016). Tamoxifen resistance is either present before the treatment (*de novo* resistance), which is nonresponsive to tamoxifen